Supporting Information

Hochstrasser et al. 10.1073/pnas.1405079111

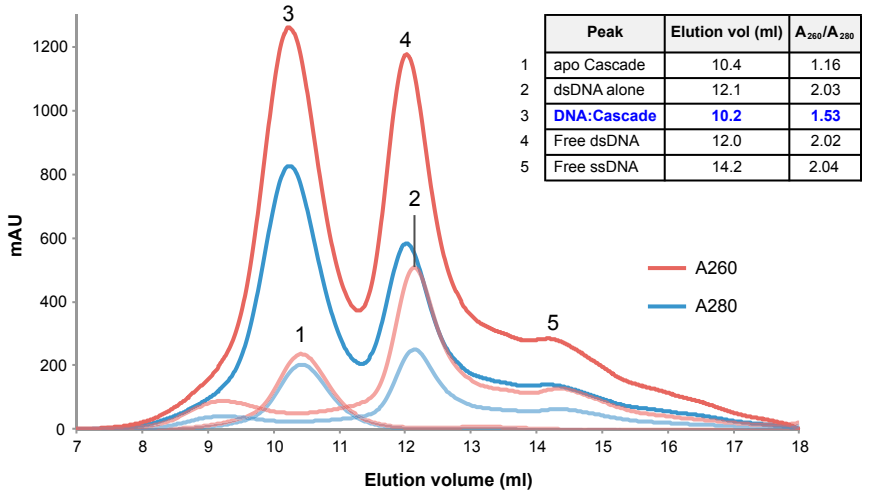

	Peak	Elution vol (ml)	A_{260}/A_{280}
1	apo Cascade	10.4	1.16
2	dsDNA alone	12.1	2.03
3	**DNA:Cascade**	**10.2**	**1.53**
4	Free dsDNA	12.0	2.02
5	Free ssDNA	14.2	2.04

Fig. S1. Size-exclusion run to remove unbound DNA after reconstituting DNA–Cascade (CRISPR-associated complex for antiviral defense; CRISPR, clustered regularly interspaced short palindromic repeats) for EM. Cascade was incubated with a 2× molar excess of target dsDNA at 37 °C before injection onto a Superdex 200 size-exclusion column. Free DNA elutes at about 12 mL and is easily separable from DNA–Cascade, which elutes after 10.4 mL. This peak was pooled, concentrated, and analyzed by cryoEM. mAU, milliabsorbance units.

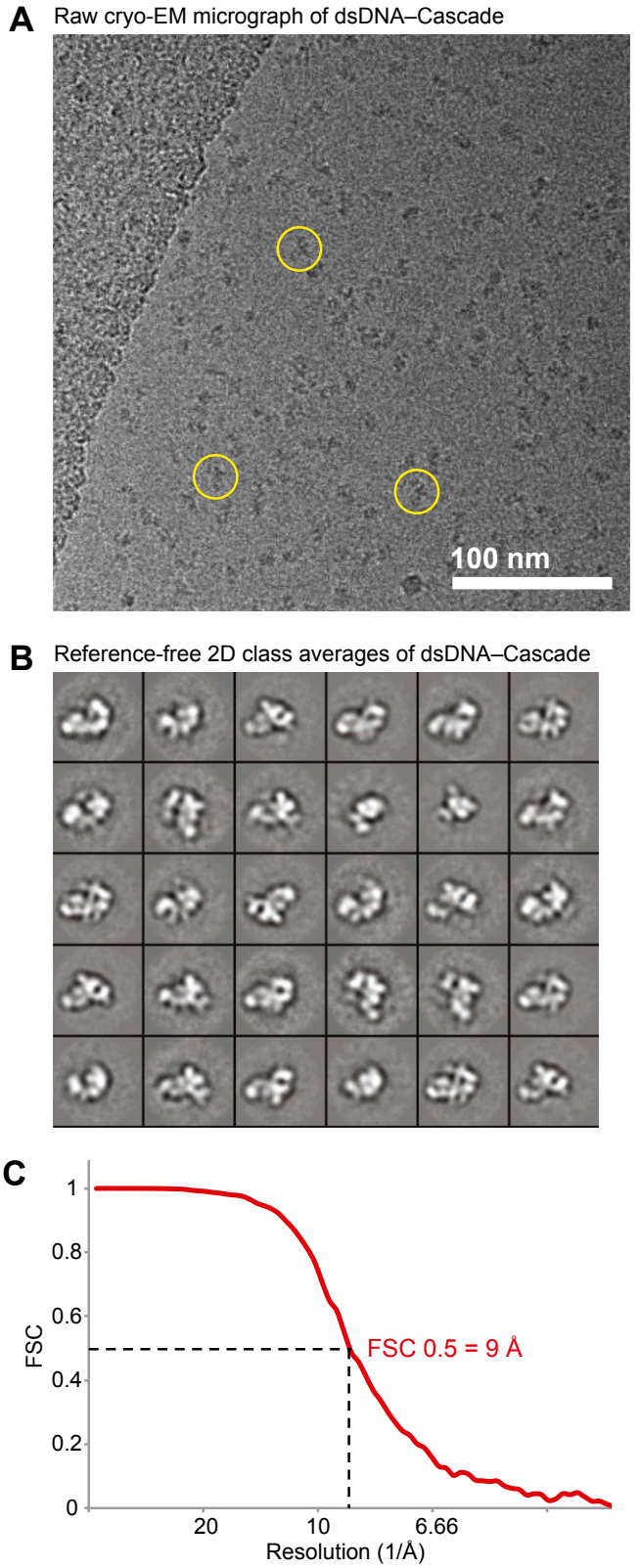

Fig. S2. Molecular architecture of dsDNA-bound Cascade. (*A*) Raw cryoEM micrograph of dsDNA-bound Cascade. (Scale bar, 100 nm.) (*B*) Representative reference-free 2D class averages of dsDNA-bound Cascade. The width of the boxes is ~314 Å. (*C*) Fourier shell correlation (FSC) curve for the final reconstruction, showing the resolution to be ~9 Å using the 0.5 FSC criterion.

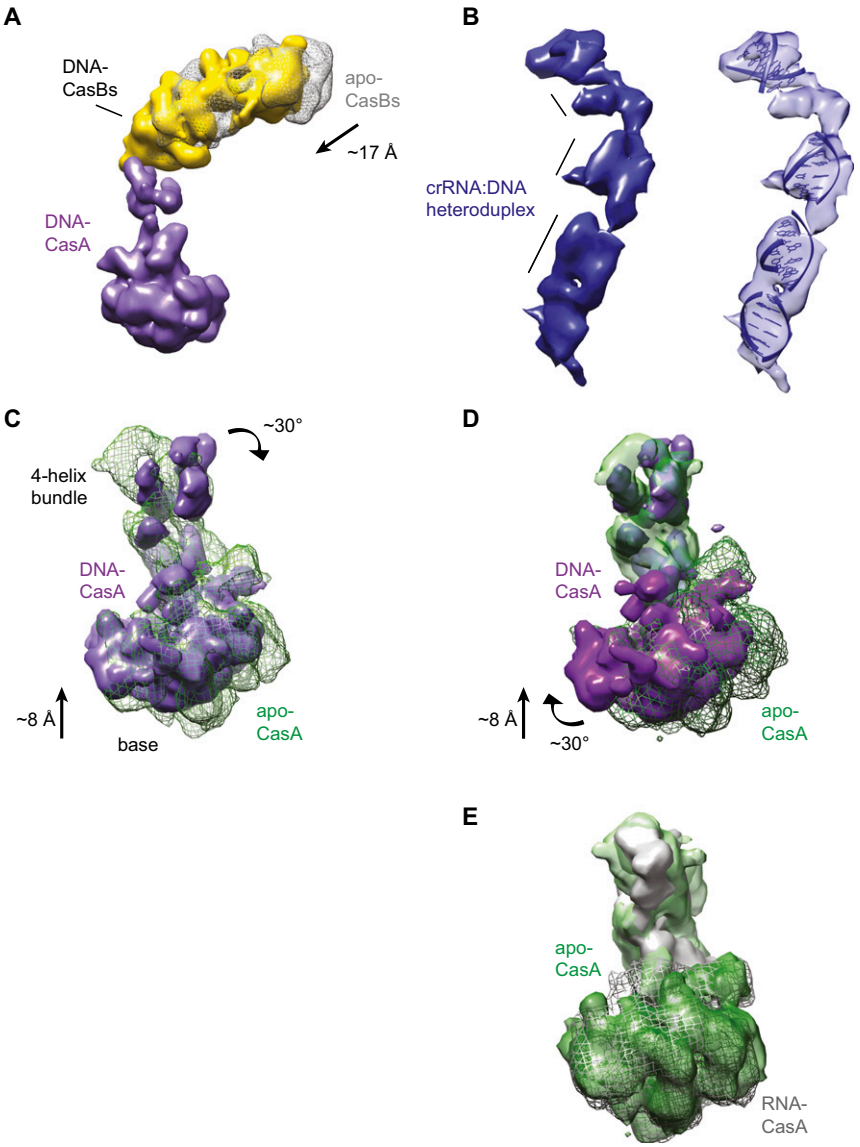

Fig. S3. Comparison of subunits between Cascade structures. (*A*) CasB1 and CasB2 from the dsDNA-bound Cascade (DNA-CasBs, yellow) overlaid on CasB1 and CasB2 from apo-Cascade (apo-CasBs, gray mesh) after alignment based on optimal cross-correlation between the CasC backbones of the two structures. The arrow denotes translation of the DNA–CasBs relative to apo-CasBs. CasA from the dsDNA-bound Cascade (purple surface) is shown for reference. (*B*) (*Left*) CRISPR (cr)RNA–DNA heteroduplex segmented from the dsDNA-bound Cascade structure showing several segments of double-stranded density marked by black lines. (*Right*) Five-base-pair segments of modeled dsDNA docked into this segmented crRNA–DNA heteroduplex density. (*C*) CasA density from the dsDNA-bound Cascade reconstruction (DNA–CasA, purple surface) overlaid on the CasA density from the previously reported apo-Cascade cryoEM reconstruction (apo-CasA, green mesh) after alignment based on optimal cross-correlation between the CasC backbones of the two structures. Arrows denote rotation or translation of the four-helix bundle (4-helix bundle) and base (base) of DNA-CasA relative to those domains of apo-CasA. (*D*) The four-helix bundle of CasA from apo-Cascade (light green surface) was aligned to the four-helix bundle in the dsDNA-bound Cascade (light purple surface) based on optimal cross-correlation. The base of CasA from apo-Cascade (dark green mesh) was transformed based on these alignment parameters. Arrows denote the rotation and translation of the base of DNA–CasA (dark purple surface) still needed to optimally align the bases of these two structures. (*E*) The four-helix bundle of CasA from apo-Cascade (light green surface) was aligned to the four-helix bundle in the ssRNA-bound Cascade (light gray surface) based on optimal cross-correlation. The base of CasA from apo-Cascade (dark gray mesh) was transformed based on these alignment parameters. There is no additional translation or rotation needed to align the bases, indicating that the entire CasA subunit rotates as a rigid body.

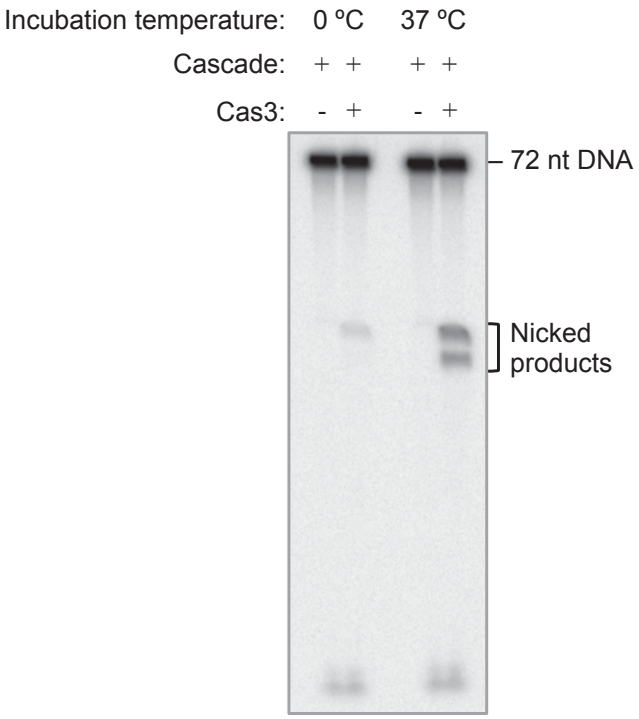

Fig. S4. Denaturing gel showing that Cas3 cleavage of a Cascade-bound DNA target is impaired when the reaction is kept on ice (0 °C). [^{32}P]DNA (1 nM) was preincubated with 1 μM Cascade at 37 °C before addition of 500 nM maltose-binding protein (MBP)-Cas3. Reactions were incubated either on ice or at 37 °C for 1 h before product resolution on a 10% urea/PAGE gel.

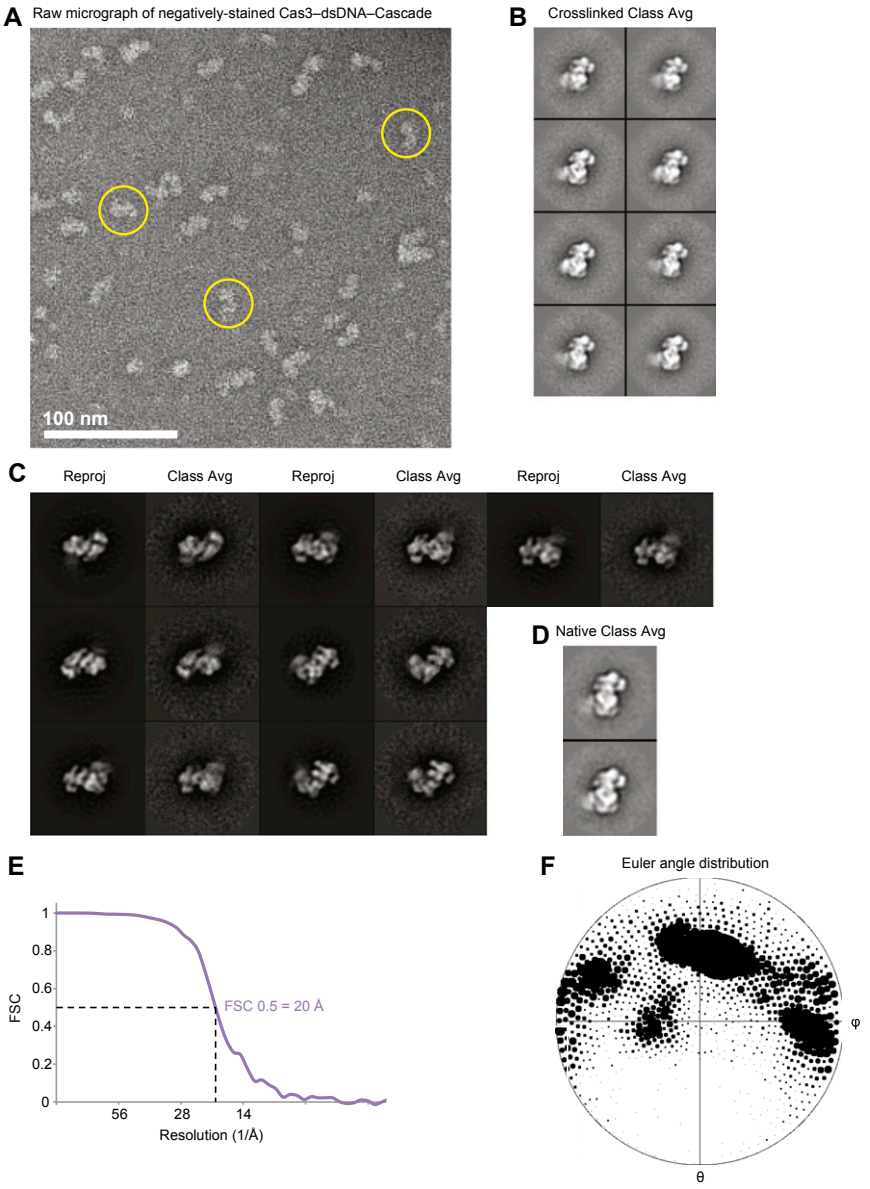

Fig. S5. Molecular architecture of Cas3–dsDNA–Cascade. (*A*) Representative raw untilted micrograph of negatively stained, cross-linked Cas3–dsDNA–Cascade. (Scale bar, 100 nm.) Several particles are outlined with yellow circles. (*B*) Reference-free 2D class averages of cross-linked Cas3–dsDNA–Cascade include an additional globular density corresponding to Cas3. The width of the boxes is ∼404 Å. (*C*) Reference-free 2D class averages of cross-linked Cas3–Cascade–dsDNA (second, fourth, and sixth columns) matched to reprojections of the final reconstruction (first, third, and fifth columns). The width of the boxes is ∼404 Å. (*D*) Representative reference-free 2D class averages of native Cas3–dsDNA–Cascade. The width of the boxes is ∼404 Å. (*E*) FSC curve for the final reconstruction, showing the resolution to be ∼20 Å using the 0.5 FSC criterion. (*F*) Euler angle distribution for the final reconstruction.

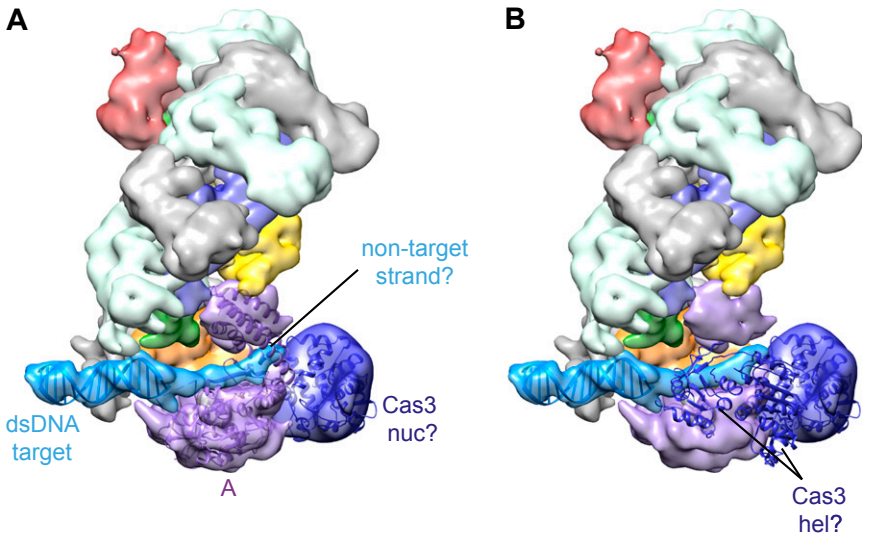

Fig. S6. Cas3 domain modeling suggests the non-target strand could extend off the end of the duplex into Cas3's nuclease domain. (*A*) Cas3 density from the negative-stain reconstruction mapped onto the cryoEM reconstruction of dsDNA-bound Cascade as in Fig. 2*B*. Notably, there is a long, tube-shaped density (non-target strand) extending from the duplex (dsDNA target) with only minor steric clashes with the crystal structure of CasA. It is difficult to determine unambiguously whether this segment is DNA or protein, so in the main text it is conservatively assigned as part of CasA. In this alternative segmentation, it has been assigned as part of the DNA. We speculate that all or part of this density could be a portion of the non-target strand being directed toward the site of Cas3 association. Additionally, a Phyre homology model of the *Escherichia coli* Cas3 nuclease domain (Cas3 nuc) is docked into the experimental Cas3 density to show that the general size and shape of this domain agree well with the experimental density. (*B*) A Phyre homology model of the helicase domain (Cas3 hel) is modeled onto the structure for further size comparison, although its precise placement is entirely theoretical.

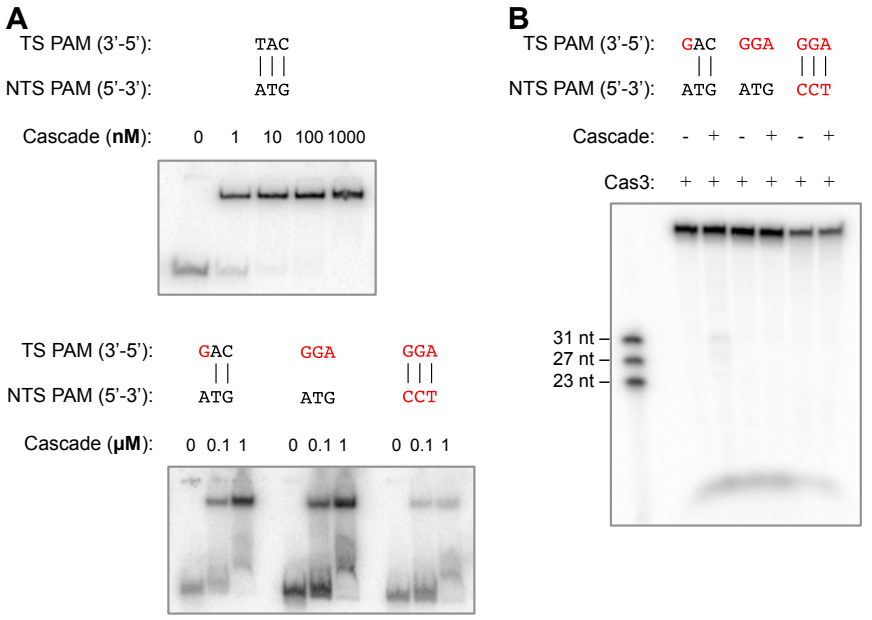

Fig. S7. Altering the protospacer adjacent motif (PAM) sequence on the target strand causes severe binding and cleavage defects. (*A*) Native gel electrophoretic mobility-shift assays showing that dsDNA substrates with mutations to the target strand PAM sequence are poorly bound by Cascade compared with those with an intact PAM, even at high protein concentration. An increasing concentration of Cascade was incubated with 0.2–0.5 nM ^{32}P-labeled dsDNA at 37 °C for 30 min in 1× reaction buffer [20 mM Hepes (pH 7.5), 100 mM KCl, 5% glycerol, 100 μM $NiCl_2$, and 5 mM $MgCl_2$]. Bound and unbound species were resolved at 4 °C on a 6% native polyacrylamide gel. NTS, non-target strand; TS, target strand. (*B*) Denaturing gel showing that the dsDNA targets in *A* are not cleaved in the presence of 500 nM MBP-Cas3 and 1 μM Cascade in the same buffer. The cleavage reaction proceeded for 30 min at 37 °C before analysis by 10% urea/PAGE.

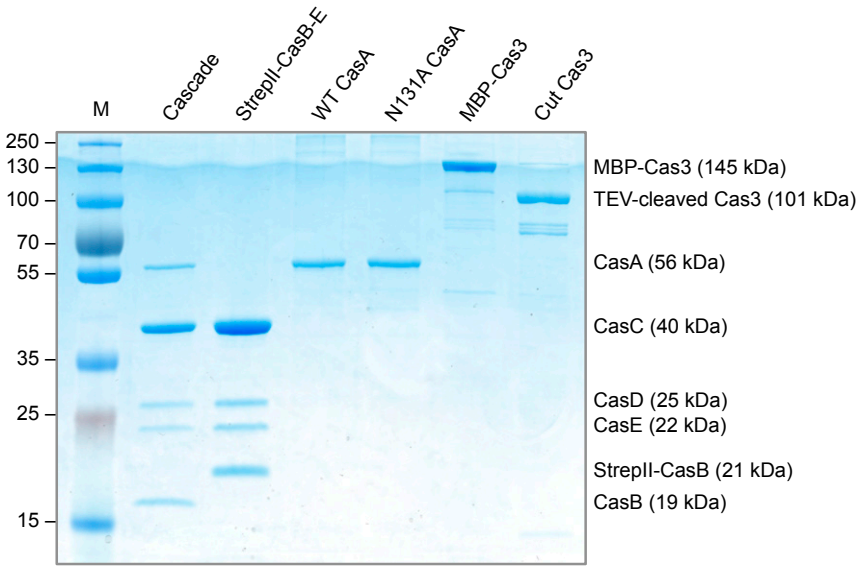

Fig. S8. SDS/PAGE depicting all proteins used in this study.

Table S1. DNA oligomers used in this study

Purpose	Oligomer	Sequence (5′-3′)	Description
Structural studies; cleavage and binding assays	MLH-46	CATGAGGTCCCTCGTTTAGTCTGTTGGCAAGCCAGGATCTGAACAATACCGTCATCGGAGGTACGATCAAGG	R44 protospacer/ATG PAM target strand
	MLH-47	CCTTGATCGTACCTCCGATGACGGTATTGTTCAGATCCTGGCTTGCCAACAGACTAAACGAGGGACCTCATG	R44 protospacer/ATG PAM non-target strand
Cleavage and binding assays	MLH-282	CATGAGGTCCCTCGTTTAGTCTGTTGGCAAGCCAGGATCTGAACAATACCGTCTTCGGAGGTACGATCAAGG	R44 protospacer/AAG PAM target strand
	MLH-283	CCTTGATCGTACCTCCGAAGACGGTATTGTTCAGATCCTGGCTTGCCAACAGACTAAACGAGGGACCTCATG	R44 protospacer/AAG PAM non-target strand
	MLH-284	CATGAGGTCCCTCGTTTAGTCTGTTGGCAAGCCAGGATCTGAACAATACCGTCCTCGGAGGTACGATCAAGG	R44 protospacer/AGG PAM target strand
	MLH-285	CCTTGATCGTACCTCCGAGGACGGTATTGTTCAGATCCTGGCTTGCCAACAGACTAAACGAGGGACCTCATG	R44 protospacer/AGG PAM non-target strand
	MLH-286	CATGAGGTCCCTCGTTTAGTCTGTTGGCAAGCCAGGATCTGAACAATACCGTCTCCGGAGGTACGATCAAGG	R44 protospacer/GAG PAM target strand
	MLH-287	CCTTGATCGTACCTCCGGAGACGGTATTGTTCAGATCCTGGCTTGCCAACAGACTAAACGAGGGACCTCATG	R44 protospacer/GAG PAM non-target strand
	MLH-249	CATGAGGTCCCTCGTTTAGTCTGTTGGCAAGCCAGGATCTGAACAATACCGTAGGCGGAGGTACGATCAAGG	R44 protospacer/CCT PAM target strand
	MLH-250	CCTTGATCGTACCTCCGCCTACGGTATTGTTCAGATCCTGGCTTGCCAACAGACTAAACGAGGGACCTCATG	R44 protospacer/CCT PAM non-target strand
	MLH-275	CATGAGGTCCCTCGTTTAGTCTGTTGGCAAGCCAGGATCTGAACAATACCGTCAGCGGAGGTACGATCAAGG	R44 protospacer/CTG PAM target strand
	MLH-276	CCTTGATCGTACCTCCGCTGACGGTATTGTTCAGATCCTGGCTTGCCAACAGACTAAACGAGGGACCTCATG	R44 protospacer/CTG PAM non-target strand
Cas3 plasmid construction	SHS-315	CGTAGCGGCGCCATGGAACCTTTTAAATATATATGCC	KasI + Cas3 fragment forward primer
	SHS-316	CGTAGCCTCGAGTTATTTGGGATTTGCAGGG	Cas3 fragment + XhoI reverse primer

Underlined text indicates the PAM sequence. Red text indicates a nucleotide mutation that changes the PAM to a sequence other than one of the four functional motifs. Blue text indicates the complementary (target strand) protospacer sequence. Purple text indicates the noncomplementary (non-target strand) protospacer sequence.

Table S2. Equilibrium dissociation constants between Cascade and duplexes tested in this study

Oligomer pair	PAM sequence	K_d ± SD, nM
MLH-46 + MLH-47	3′-TAC-5′ ||| 5′-ATG-3′	0.82 ± 0.14
MLH-46 + MLH-276	TAC || CTG	0.81 ± 0.33
MLH-282 + MLH-47	TTC || ATG	1.0 ± 0.6
MLH-46 + MLH-287	TAC | GAG	30 ± 6
MLH-49 + MLH-250	TAC CCT	3.8 ± 1.4

Red text indicates a nucleotide mutation that changes the PAM to a sequence other than one of the four functional motifs.

Table S3. Plasmids used in this study

Plasmid	Name	Description	Restriction sites	Primers	Source
1	pWUR547	R44 CRISPR, 7× spacer number 2 (P7) in pACYCDuet-1 expression vector	—	—	(1)
2	pWUR480	*casB* with N-terminal Strep-tag II, *casC*, *casD* in pET-52b expression vector	—	—	(2)
3	pWUR404	*casE* in pCDF-1b expression vector, no tags	—	—	(2)
4	pWUR408	*casA* in pRSF-1b expression vector, no tags	—	—	(2)
5	EcCasA-pSV272	WT *casA* expression vector with N-terminal His_6-MBP-TEV protease site tag	—	—	(3)
6	EcCasA N131A-pSV272	N131A *casA* expression vector with N-terminal His_6-MBP-TEV protease site tag	—	—	(3)
7	EcCas3-pSV272	*cas3* expression vector with N-terminal His_6-MBP-TEV protease site tag	KasI + XhoI	SHS-315 + 316	This study

TEV, tobacco etch virus.

1. Jore MM, et al. (2011) Structural basis for CRISPR RNA-guided DNA recognition by Cascade. *Nat Struct Mol Biol* 18(5):529–536.
2. Brouns SJJ, et al. (2008) Small CRISPR RNAs guide antiviral defense in prokaryotes. *Science* 321(5891):960–964.
3. Sashital DG, Wiedenheft B, Doudna JA (2012) Mechanism of foreign DNA selection in a bacterial adaptive immune system. *Mol Cell* 46(5):606–615.